International Journal of Innovative Technology and Exploring Engineering (IJITEE)
ISSN: 2278-3075 (Online), Volume-9 Issue-9, July 2020

Properties of Linear Low Density Polyethylene

Shixaliyev Kerem Seyfi, Amirov Fariz Ali

Abstract: ***As result of the modification of polyolefin, composite materials based on them were obtained for the use in special equipment in order to entrain their heat resistance. Data analysis DTA (differential thermal analysis) of the DTA curve of this polyethylene sample suggests a bimodal nature of their MWD (molecular weight distribution) which differs from polyethylene with unimodal MWD and a series of endo oxidation effects with a maximum temperature of 245, 335, 358 and 435 °C. X-ray structural studies showed that the crystal system and the size of the unit cells of the crystal lattice of LLDPE practically does not differ from those of LDPE. LLDPE as well as LDPE and HDPE has a layered structure with dense packing of macromolecules. In terms of crystallinity and crystallite sizes, LLDPE are on par with HDPE and significantly differ from LDPE. These data are in agreement with published data. The parameters of the unit cells of the crystal structure of UHMWPE are close to those of LLDPE, and by crystallinity it occupies middle ground between HDPE and LLDPE.***

Key words: linear low density polyethylene (LLDPE), LLDPE-1 - ethylene-hexene-1 copolymer, LLDPE-2 -- ethylene-octene-1 copolymer, LLDPE-3 -- ethylene-decene-1 copolymer, supramolecular polyethylene (SMPE), EHC -- copolymer of ethylene with hexane, EOC -- copolymer of ethylene with octane, NMR -- nuclear magnetic resonance, TG -- thermogravimetric, MWD -- molecular weight distribution, Vinylidene groups, composition, aging

I. INTRODUCTION

Linear low density polyethylene (LLDPE) is synthesized in the presence of a titanium-chromium catalyst and differs from each other by the length of the side branch. LLDPE-1 is a copolymer of ethylene with hexene-1, where the butyl groups (-CH_2- CH_2- CH_2- CH_3) are side branches; LLDPE-2 is a copolymer of ethylene with octene-1, where the side branches are hexyl groups: (-CH_2- $(CH_2)_3$- CH_2- CH_3); LLDPE-3 is a copolymer of ethylene with decene-1, where the side branches are octal groups: (-CH_2-($CH_2)_5$- CH_2- CH_3). With a constant composition of the copolymer, a relationship is found between the degree of crystallinity and the length of the hydrocarbon chain of the commoner. Namely, with an increase in the chain length of the commoner and, accordingly, the length of the branches from the macro chain, the effect of decreasing crystallinity increases and reaches a maximum when using α-olefins C_4-C_6 as commoners.A further increase in the chain length of α-olefins does not cause a significant decrease in the degree of crystallinity and even leads to a slight decrease in the effect of disruption of the crystal structure [1-15].

II. RESULT

Thus, by varying the degree of crystalline LLDPE by introducing more or less commoner, materials with new properties can be obtained. Unlike low density polyethylene, obtained at high pressure, the structure of which is characterized by the content of side branches of various lengths, LLDPE obtained at low pressure (up to 4.0 MPa) contains the same type of side branches. Moreover, the size of the latter, as indicated above, depending on the commoners, can vary from C_4 to C_8, in the case of LLDPE-1 and LLDPE-3, where α-C_6 and α-C_{10} were used as comonomers, respectively. This is a fundamentally important difference between LLDPE and LDPE and it largely determines a set of exceptionally high performance properties of LLDPE. Fig.1 presents a schematic representation of the structure of LDPE, LLDPE and HDPE.

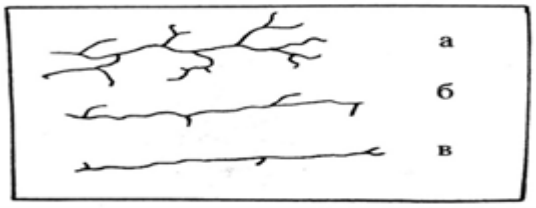

Fig. 1. Schematic illustration of the structure of LDPE - a, LLDPE - b and HDPE - c.

In terms of structural characteristics, LLDPE is close to HDPE and significantly differs from LDPE. Violation of the linear structure of polyethylene is long and short-side chains and olefin saturation. Despite their small content in the general structure of linear polyethylene they have a significant impact on the physicochemical properties of the polymer [16-25].

III. DISCUSSION

The results of an IR analysis of the structure of the synthesized LLDPEs show that the main saturated groups in the structure of LLDPE are vinyl, vinylidene and trans-vinyl groups (Table 1). The increase in the content of commoner in the composition of LLDPE leads to an increase in vinylidene groups. In all circumstances, an increase in the commoner in the composition of the copolymer (LLDPE) leads to an increase in the amount of -CH_3 groups. The content of individual fragments in the structure of LLDPE was also determined by appropriate processing of the NMR spectra of various types of LLDPE.

Revised Manuscript Received on July 30, 2020.
***** Correspondence Author
Shixaliyev Kerem Seyfi*, Azerbaijan State Oil and Industry University Baku, AZ1010, Azerbaijan, 20 Azadlig Avenue
Amirov Fariz Ali, Azerbaijan State Oil and Industry University Baku, AZ1010, Azerbaijan, 20 Azadlig Avenue.Email kerem_shixaliyev@mail.ru

Table 1
Structural characteristics of LLDPE (Synthesis conditions: temperature -160 ° C; pressure - 20 MPa; duration - 60 min; catalyst - titanium-chromium)

The monomers content in the copolymer, mole%	Σ C=C per 1000 C atoms	Vinylidene groups, %	Vinyl groups,%	Trans vinyl groups,%	$-CH_3-$ per 1000 C atoms
LLDPE -1 (EHC-1)					
0,08	0,24	10	83,5	6,5	0,05
0,150	0,25	10,2	84,3	5,5	0,07
0,450	0,42	9,8	82,9	8,1	0,21
1,10	0,44	15	76,6	8,4	0,51
1,50	0,57	25	60,9	14,1	0,65
LLDPE -2	0,40	5,9	90,1	4	0,05
(EOC-1)					
0,10	0,37	4,1	90,9	5	0,09
0,144	0,45	16,0	76	8	0,37
0,54	0,55	19,0	68	13	0,55
1,40	0,41	28,0	67	15	0,85
LLDPE -3 (EDC-1)					
0,15	0,25	10,4	85,1	4,3	0,09
0,88	0,38	14	73	13	0,51
1,67	0,39	26	55	19	0,8

The results of the quantitative determination of individual fragments of the structure of LLDPE obtained from NMR spectroscopy are compiled in Table 2.

Table 2
NMR spectroscopy data

Samples	The number of groups per 1000 C atoms			
	-CH	$-CH_2$	$-CH_3$	The commoner content in the reaction zone, mole%
LLDPE -1	3,3	93,4	3,3	0,1
LLDPE -2	4,4	91,2	4,4	0,1
LLDPE -3	6,2	87,6	6,2	0,2

The main fragment of the LLDPE structure are $–CH_2$ -- groups. The number of –CH -- groups is on par with the $–CH_3$ group. Because of the low content of olefin saturation in the NMR spectrum, it was not possible to detect the presence of unsaturated groups. The latter in the structure of LLDPE were determined by the IR method. Based on the IR and NMR spectroscopic data, the structure of LLDPE can be represented as follows

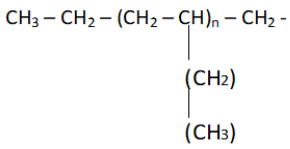

With an increase in commoner content in copolymer an increase in the CH_3 groups shows that the commoner in the copolymer is distributed by separate units and the distribution is statistical in nature. The lack of large blocks of commoner in LLDPE is also shown by derivatographic data. Block copolymers are usually characterized by two melting points whereas copolymers with a statistical distribution of copolymers in the composition are characterized by the same melting point, but differ from the melting point of photopolymers [10 - 20]. Fig. 2 shows the derivatographic - DTA curves of LLDPE. For comparison, DTA curves of HDPE, UHMWPE and LDPE are presented here.

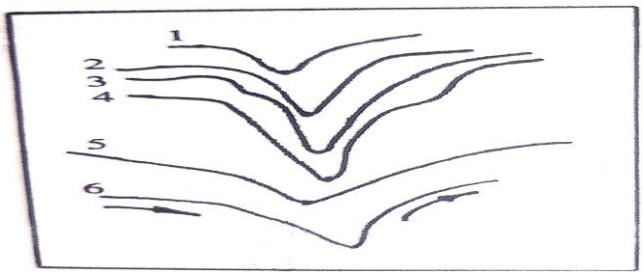

Fig. 2. DTA curves: (1) - LDPE (T_m - 110 °C), (2) – HDPE (T_m - 118), 3) - LLDPE-1 (T_m - 127 °C), (4) - LLDPE-2 (T_m - 132 °C), (5) -LLDPE-3 (T_m - 129 °C), (6) - UHMWPE (T_m - 141 °C).

Analysis of the DTA curves shows that all samples of polyethylene are characterized by the same melting point. NMR spectroscopy data confirmed that in the composition of LLDPE synthesized in the presence of a titanium-chromium catalyst, the commoner distribution is statistical in nature and the mechanism of formation of LLDPE-1, LLDPE-2, LLDPE-3 in the presence of this catalyst remains almost the same and in all cases regardless of the synthesis conditions (Table 2), the commoner in the copolymer composition is distributed according to the law of the case.

Figure 3 shows the derivatographic curves of HDPE synthesized in solution in the presence of a titanium-chromium catalyst.

This HDPE sample is characterized by sufficiently high thermophysical properties. The melting point is 132 °C, the oxidation temperature is 245 °C and temperature of 50 % of weight loss is 480 °C.

From the TG curve of the dependence of the mass loss (Δm) of polymer on temperature (T) it is evident that this curve has two distinct temperature regions at which polyethylene, when heated, noticeably loses weight.

These regions correspond to temperatures of 310 – 370 ° C and 370 – 420 ° C, respectively.

This type of TG curve is characteristic of polymer samples predominantly with bimodal MWD.

The TG curve of polyethylene with a unimodal MWD distribution, as a rule, is characterized by a single temperature region at which polyolefins .

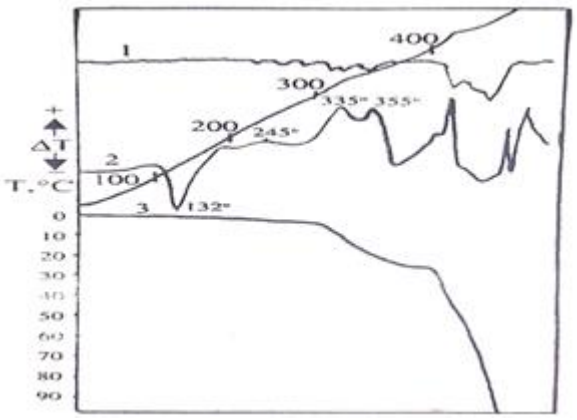

Fig. 3. Derivatogram of linear low density polyethylene, 1-DTG, 2-DTD, 3-TG curves

DTA data analysis of these polyethylene samples suggests a bimodal nature of their MWD which differ from polyethylene with unimodal MWD a series of oxidation endo-effects with a maximum temperature of 245, 335, 358, and 435 °C. X-ray diffraction studies have shown that the crystal system and the size of the unit cells of the crystal lattice of LLDPE practically does not differ from those of LDPE. LLDPE as well as LDPE and HDPE has a layered structure with dense packing of macromolecules. However, in contrast to LDPE, in which the presence of lateral branches of different lengths causes disordering of its crystals, the crystals in LLDPE are more ideal, and the crystals are large in size, therefore, even with the same density T_m of LLDPE is always higher than LDPE. It is also noteworthy that in the LLDPE crystals between its layers, there are chains of the same type of lateral branches characteristic only for LLDPE. This structural feature of LLDPE gives products obtained on their basis (in particular thin films) higher tensile strength compared to LDPE.

Table 3

Table of unit cell parameters and crystallite size for various types of polyethylene

Samples	“a”	“b”	“c”	L, A	Crystallinity, %
LLDPE -1	7,45	4,87	2,53	151,5	68
LLDPE -2	7,47	4,97	2,53	151,5	67
LLDPE -3	7,50	4,87	2,53	154,5	64
High density polyethylene (HDPE)	7,45	4,97	2,53	150,5	70
Low density polyethylene(LDPE)	7,45	4,91	2,53	117	45
Ultra-high molecular weight polyethylene, (UHMW PE)	7,45	4,90	2,53	145	60

The dependence of the change in specific volume on the temperature of polyethylene is characterized by different values of V at a given T. The dependence of the change in V on T in LLDPE is quite different from other polyolefin. Namely, if we draw straight lines along the points of the upper branch of the dilatometry cooling curve, then we get two sections ~ 120 to 165 °C and from 165 to 230 °C (Fig. 4).

Apparently, upon cooling the LLDPE melt to the crystallization temperature, their macromolecules are partially ordered at higher temperatures. The indicated two sections of the upper branch of the dilatometry cooling curve of LLDPE are related to the nature and characteristics of the same type of lateral branches.

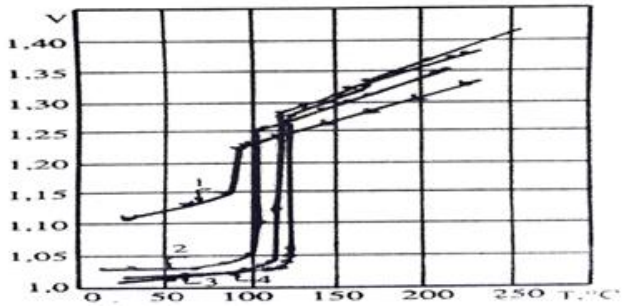

Fig. 4. The dependence of the change in specific volume (V) on temperature for: 1-LDPE; 2-HDPE; 3-LLDPE-2 and 4-LLDPE-3.

It is expected that during cooling of the LLDPE melt, namely, the EOC-1 and EDC-1 copolymer, the formation of microcrystalline regions precedes the beginning of their crystallization due to the laying of similar lateral branches having copolymers in the structure. Microcrystalline areas formed due to lateral branches concentrate along the main chain and lead to an increase in the strength properties and resistance of EOC-1 and EDC-1 to cracking.

An analysis of the rheological characteristics of polyethylene's with a MFR equal to 1,4–7,0 g/10 min in the temperature range 135–300 ℃ showed that in these temperature ranges the efficiency of the polymer melt viscosity varies slightly with temperature. The transition of HDPE to the plateau of a highly elastic state, at a certain critical level of the dynamic loss modulus (E′ and E″) occurs clearly and E'_m and E''_{max} have the same values. The maximum value of $E_{max} = 7{,}28 \cdot 10^9$ N/m^2 is a measure of the stiffness of a fully crystalline polymer.

The functional dependence of the volume dynamic modulus of elasticity of monodisperse, polydispersity and branched polyethylene's with their main parameters –M, ρ, V_m and the ultrasonic propagation velocity of the polymer showed the invariance of the E_y-ρ dependence for polyethylene's. With repeated loading and unloading of polyethylene samples, a known hysteresis pattern is revealed. Samples of polyethylene's with MW up to $2{,}5 \cdot 10^4$ are brittle and break down under primary loading. With increasing MW, the number of possible loading cycles before fracture of the samples at the beginning grows and then decreases, the apparent strength (σρ) grows, although its limiting values are less than that with stationary deformation.

Another feature of hysterisation of polyethylene is the complete restoration of strength during repeated cycles. Heat treatment has a significant impact on the bulk properties of polyethylene.

With prolonged exposure of the polymer at high temperatures due to the simultaneous passage of crystallization, recrystallization, structuring, or partial destruction, the temperature dependence of the density changes significantly.

At 200–250 ℃ crystallization is suppressed, the packing density of macromolecules decreases, and at room temperature samples with values of ρ 850 ÷760 kg/m^3 are obtained. In the temperature regions T_{cr} and T_m, their narrow temperature range is observed, and the smaller the MFR, the more V_{sp} and the less ρ.

IV. CONSLUSION

The density of polyethylene samples strongly depends on the cooling rate, T_g increases from -106 ℃ to 62 ℃ with increasing cooling rate.

With an increase in MFR, a pronounced induction period of crystallization is manifested. In general, the crystallization mechanism of single crystals and polymer obtained from the melt differs slightly.

The dependence of the fraction of free volume on T-T_g presents an opportunity at any T and cooling rate to determine the value of V_{sp} or ρ, which proves the invariance of the results with respect to temperature.

The generalized temperature invariant characteristic is established for the most important physical properties of linear polyethylene's - V_{sp}, V_f, f_f, coefficient of volumetric thermal expansion, etc. The effect of polydispersity of polyethylene's on their properties has shown that the smaller the MW value, the higher the values of shear rates R_{max} (M) appears (the value of rheological functions in MW). Low-molecular weight polyethylene samples are characterized by a narrower MW. With increasing MW, the position of R_{max}(M) shifts toward ever smaller values of γ, and the value of R_{max} (M) decreases, i.e., there is a typical pattern of a wide distribution of MW. Narrow MWD polyethylene is characterized by a minimum value of the generalized rheological index of polydispersity RPI and for monodispersed polyethylene, the RPI value is zero. In the DTA curve of the HDPE in the region of 300℃ and above, a series of exon- and endo-effects are observed that relate to oxidative degradation, and above 300℃, molecular chains broken -- MW decreases, at more than 360℃, the formation of volatile decomposition products begins and at 475℃ deep decomposition of polymer occurs.

Narrow fractions of HDPE with $M_w/M_n \approx 1{,}02$, in contrast to the basic samples of polyethylene have a smaller T_m interval and at a value of MW from $3 \cdot 10^3$ to $5 \cdot 10^5$, do not depend on MW. The dependence of the thermal properties of HDPE on MW is large-scale and seems to be grouped in a certain MW interval, with increasing MW, the T_m interval expands and the overall rate of thermal oxidation and destruction increases.

The formation mechanism of LLDPE in the presence of a titanium-chromium catalyst with hexene-1 (LLDPE-1), octene-1 (LLDPE-2) and decene-1 (LLDPE-3) is practically the same and the distribution of the commoner in the composition of the copolymer occurs according to the law of the case.

LLDPEs are characterized by high thermophysical properties $T_m = 132^0$C and temperature of 50 % of weight loss is 480° C. LLDPE with a close degree of crystallization (0,64-0,68) and crystallite sizes (151-154 Å) has a higher tensile strength compared to LDPE. Depending on the MW the maximum conversion to a crystalline state at a given temperature for narrow LLDPE fractions can be 0,50 for a high molecular weight sample and up to 0,85 for a low molecular weight sample

An analysis of the rheological properties of LLDPE at 190–250 °C and shear stress of $10^2 \div 10^4$ MPa showed that at the same temperatures the dependence logγ/logτ for the copolymers is the same and the reduced viscosity is independent of temperature. LLDPE can be processed by almost all known processing methods for thermoplastics.

The presence in the structure of LLDPE of the same type and rather long lateral branches affects the permeability. Polymer films were obtained by pressing LLDPE at 180° C for 400 hours. At room temperature HDPE had a high vapor permeability. This is attributable to the relatively low density and crystallinity of LLDPE.

REFERENCES

1. B. Huang and J. Liu, "The effect of loading rate on the behavior of samples composed of coal and rock," International Journal of Rock Mechanics and Mining Sciences, vol. 61, pp. 23–30, 2013
2. J. Liu, E. Wang, D. Song, S. Wang, and Y. Nia, "Effect of rock strength on failure mode and mechanical behavior of composite samples," Arabian Journal of Geosciences, vol. 8, no. 7, pp. 4527–4539, 2015.
3. S. Chen, D. Yin, F. Cao, Y. Liu, and K. Ren, "An overview of integrated surface subsidence-reducing technology in mining areas of China," Natural Hazards, vol. 81, no. 2, pp. 1129–1145, 2016.
4. C.P. Lu, G.J. Liu, Y. Liu, N. Zhang, J.H. Xu, and L. Zhang, "Micro seismic multi-parameter characteristics of rock burst hazards induced by hard roof fall and high stress concentration," International Journal of Rock Mechanics and Mining Sciences, vol. 76, pp. 18–32, 2015.
5. S. Chen, D. Yin, N. Jiang, F. Wang, and Z. Zhao, "Mechanical properties of oil shale-coal composite samples," International Journal of Rock Mechanics and Mining Sciences, vol. 123, p. 104120, 2019.
6. S. J. Chen, D. W. Yin, H. M. Liu, B. Chen, and N. Jiang, "Effects of coal's initial macro cracks on rock burst tendency of rock–coal composite samples," Royal Society Open Science, vol. 6, no. 11, Article ID 181795, 2019.
7. R.-H. Cao, P. Cao, H. Lin, C. Z. Pu, and K. Our, "Mechanical behavior of brittle rock-like specimens with pre-existing fissures under uniaxial loading, experimental studies and particle mechanics approach," Rock Mechanics and Rock Engineering, vol. 49, no. 3, pp. 763–783, 2016.
8. X. L. Li, L. J. Kang, H. Y. Li, and Z. H. Ouyang, "Three-dimensional numerical simulation of bust-prone experiments about coal-rock combination," Journal of China Coal Society, vol. 36, no. 12, pp. 2064–2067, 2011.
9. D. W. Yin, S. J. Chen, X. Q. Liu, and H. F. Ma, "Effect of joint angle in coal on failure mechanical behavior of roof rock-coal combined body," Quarterly Journal of Engineering Geology and Hydrogeology, vol. 51, no. 2, pp. 202–209, 2018.
10. D. W. Yin, S. J. Chen, B. Chen, X. Q. Liu, and H. F. Ma, "Strength and failure characteristics of the rock-coal combined body with single joint in coal," Geotechnics and Engineering, vol. 15, no. 5, pp. 1113–1124, 2018.
11. S. J. Chen, D. W. Yin, B. L. Zhang, H. F. Ma, and X. Q. Liu, "Study on mechanical characteristics and progressive failure mechanism of roof-coal pillar structure body," Chinese Journal of Rock Mechanics and Engineering, vol. 37, no. 7, pp. 1588–1598, 2017.
12. Z.-H. Zhao, W.-M. Wang, C.-Q. Dai, and J.-X. Yan, "Failure characteristics of three-body model composed of rock and coal with different strength and stiffness," Transactions of Nonferrous Metals Society of China, vol. 24, no. 5, pp. 1538–1546, 2014.
13. S. J. Chen, D. W. Yin, N. Jiang, F. Wang, and W. J. Guo, "Simulation study on effects of loading rate on uniaxial compression failure of composite rock-coal layer," Geotechnics and Engineering, vol. 17, no. 4, pp. 333–342, 2019.
14. Z. H. Zhao, W. M. Wang, L. H. Wang, and C. Q. Dai, "Compression-shear strength criterion of coal-rock combination model considering interface effect," Tunneling and Underground Space Technology, vol. 47, pp. 193–199, 2015.
15. T. B. Zhao, W. Y. Guo, C. P. Lu, and G. M. Zhao, "Failure characteristics of combined coal-rock with different interfacial angles," Geotechnics and Engineering, vol. 11, no. 3, pp. 345–359, 2016.
16. Y. L. Tan, X. S. Liu, J. G. Ning, and Y. W. Lu, "In situ investigations on failure evolution of overlying strata induced by mining multiple coal seams," Geotechnical Testing Journal, vol. 40, no. 2, pp. 244–257, 2017.
17. Y. L. Tan, X. S. Liu, B. Shen, J. G. Ning, and Q. H. Gu, "New approaches to testing and evaluating the impact capability of coal seam with hard roof and/or floor in coal mines," Geotechnics and Engineering, vol. 14, no. 4, pp. 367–376, 2018.
18. B. A. Paulsen, B. Shen, D. J. Williams, C. Huddleston-Holmes, N. Erarslan, and J. Qin, "Strength reduction on saturation of coal and coal measures rocks with implications for coal pillar strength," International Journal of Rock Mechanics and Mining Sciences, vol. 71, pp. 41–52, 2014.
19. T. Wang, Y. D. Jiang, S. J. Zhan, and C. Wang, "Frictional sliding tests on combined coal-rock samples," Journal of Rock Mechanics and Geotechnical Engineering, vol. 6, no. 3, pp. 280–286, 2014.
20. X. Qu, "Experimental study on influence of mechanical properties of roof and floor on stability of strip coal pillar," Shandong University of Science and Technology, Qingdao, China, 2018, Master's thesis.
21. Amirov F. A. Theory and practice of obtaining composite materials based on polymer mixtures (monograph Premier Publishing. S. R. O Vienna, Austria. 2018 E-mail: pub@publishing.orgconference@sibscience.ru
22. Shikhaliyev K. S. Polymer technology (Study.manual). Vol. 1. Lambert Academic Publishing, Meldrum street, Beau Bassin Riga, Latvia2018, 252p. www.ingimage.cominfo@omnisc riptum.com
23. Shikhaliyev K. Technology of polymers (Proc.benefits) Vol. 2, LAMBERT Academic Publishing, Meldrum street, Beau Bassin Riga, Latvia.2018 303p.www.ingimage.com
24. Shikhaliev K. Studying the crosslinking mechanism and structure of crosslinked polyethylene. Eurasian Union learned (ESU). U. Moscow Monthly scientific journal. 2018.-No4 (49). 3 part. pp. 73-77. E-mail: info@euroasia-science.ru.
25. Serenko O.A., Goncharuk G.P. et al. / Effect of temperature on the deformation behavior of a composite based on polypropylene and rubber particles // High Molecular Compounds.-2007.-No. 1.-P.71-78.
26. Kerem Shixaliyev. Theory and practice of obtaining composite materials based on polymer blends. Proceedings of the Fouth International Confrense of European Academy of Science BONN,GERMANY. 2019,-pp. 32-33.